Journal of Alloys and Compounds 662 (2016) 339–347

Contents lists available at ScienceDirect

Journal of Alloys and Compounds

journal homepage: http://www.elsevier.com/locate/jalcom

Microstructure, wettability, optical and electrical properties of HfO_2 thin films: Effect of oxygen partial pressure

J. Gao [a], G. He [a, *], B. Deng [a], D.Q. Xiao [a], M. Liu [b, **], P. Jin [a], C.Y. Zheng [a], Z.Q. Sun [a]

[a] School of physics and Materials Science, Radiation Detection Materials & Devices Lab, Anhui University, Hefei 230601, China
[b] Key Laboratory of Materials Physics, Anhui Key Laboratory of Nanomaterials and Nanostructure, Institute of Solid State Physics, Chinese Academy of Sciences, Hefei 230031, China

ARTICLE INFO

Article history:
Received 8 August 2015
Received in revised form
16 November 2015
Accepted 10 December 2015
Available online 12 December 2015

Keywords:
HfO_2 thin films
RF sputtering
Optical properties
Band gap
Wettability

ABSTRACT

The effect of oxygen partial pressure on the microstructure, wettability, optical and electrical properties of sputtering-derived HfO_2 thin films has been systematically investigated by using x-ray diffraction (XRD), fourier transform infrared spectroscopy (FTIR), scanning electron microscope (SEM), atomic force microscope (AFM), UV–visible spectroscopy (UV–Vis), spectroscopy ellipsometry (SE), and electrical measurements. XRD results have shown that the HfO_2 thin films are all polycrystalline with monoclinic phase. Based on analysis from FTIR, a strong absorption peak centered at 1105 cm^{-1} has been detected, indicating the formation of the interfacial layer. Reduction in particle size and decrease in root mean square (RMS) roughness of the HfO_2 thin films have been detected by SEM and AFM measurements with the increase in oxygen partial pressure. Meanwhile, the contact angle decreases and the wettability increases with increasing the oxygen partial pressure. Combined with UV–vis and SE, the optical function of HfO_2 thin films as functions of oxygen partial pressure has been determined. By means of electrical measurements, evolution of electrical performance of MOS capacitor based on HfO_2 gate dielectrics related with oxygen partial pressure has been investigated systematically.

1. Introduction

Due to its outstanding chemical stability and excellent physical properties, transition metal oxides have been paid much attention. So, it is suitable for several industrial applications in the field of electronics and optoelectronics [1]. For example, due to its high dielectric constant and wide band gap, hafnium dioxide (HfO_2) thin films have also been regarded as s a promising high-k gate dielectric material for metal-oxide-semiconductor field effect transistor (MOSFET) to replace conventional SiO_2 [2–4]. Moreover, due to its high refractive index and good mechanical, thermal and chemical properties [5,6], it is also regarded as a promising protective coatings to develop hydrophobic coatings for outdoor insulators. So, pollution attached on the surface of the insulators by various sources such as wind, nearby cement industries, industrial smoke and coastal salt can be overcome by water hydrophobic coatings. As we know, solid surfaces can be divided into two categories based on the wettability of water. The water contact angle (WCA) on a solid surface can be defined as a hydrophobic (CA>90°) or hydrophilic (CA<90°) surface [7]. The precise determination of the optical properties are an important method to measure whether that HfO_2 can be regarded as a good high-k gate dielectric material or not and the structure and hydrophobic properties are an important indicator to measure whether that HfO_2 can be looked as good surface coatings materials or not. By far, the fabrication methods for HfO_2 gate dielectrics or coatings can be categorized into three major approaches based on the reaction mechanism, namely solution deposition, chemical vapor deposition (CVD), and physical vapor deposition (PVD) [8]. Solution-based methods mainly include sol–gel, metal-organic decomposition, and so on [9–11]. Compared to the solution-based deposition and chemical vapor deposition, the advantages of PVD-based deposition method include controllable growth of the films and compositional consistency between the target and the deposited film [12–14]. Due to inherent versatility and the capability of obtaining a homogeneous surface coverage at low temperatures under controlled processing conditions [15,16], sputtering has been pursued to obtain HfO_2 thin films in current work.

* Corresponding author.
** Corresponding author.
E-mail addresses: cheriling16@126.com (G. He), mliu@issp.ac.cn (M. Liu).

http://dx.doi.org/10.1016/j.jallcom.2015.12.080
0925-8388/

As we know, there are many deposition parameters to affect the microstructure and properties of sputtering-derived thin films, such as working gas pressure [6], RF power [17] and different O_2/Ar flow ratio [18]. Much work has been devoted to controlling the working gas pressure and RF power to obtain the HfO_2 thin films with high quality. Although the effect of O_2/Ar flow ratio on HfO_2 coatings have been investigated [19–22], it is still worth to investigate systematically since that the O_2/Ar flow ratio is expected to be a key factor which affects the film's stoichiometric ratio, structure and optical properties. By far, the effect of O_2/Ar flow ratio on the stoichiometric and structural properties of sputtered-derived HfO_2 thin films has been reported by many groups [19–21]. For example, Pereira et al. [22] investigated the effect of O_2/Ar flow ratio on the dielectric and optical properties of HfO_2 thin films [22]. Although there exists so much work, the influence of O_2/Ar flow ratio on the structure, hydrophobic, optical and electrical properties of sputtering-grown HfO_2 coatings are not given completely. To investigate the morphology of HfO_2 thin films preferably, atomic force microscopy (AFM) and scanning electron microscope (SEM) have been combined. Combined with ultraviolet–visible spectroscopy (UV–Vis) and spectroscopy ellipsometry (SE) measurements, the optical constants of sputtering-derived HfO_2 thin films have been discussed as a function of oxygen partial pressure. Meanwhile, by means of *C–V* and *I–V* measurements, electrical performance of MOS capacitor based on HfO_2 gate dielectrics related with oxygen partial pressure has been investigated systematically.

2. Experiment details

First, Si (001) substrates with resistivity of 2–5 Ω/cm were cleaned by a modified RCA (Radio Corporation of American) processing method. Then, the wafers were immersed in diluted HF (1%) solution for 30s to remove any native oxide and washed by ionized water. After that, the wafers were dried by pure N_2. Finally, the Si wafers were put into vacuum chamber quickly. To explore the microstructure and optical properties of HfO_2 thin films preferably, the quartz plates were also chosen as the substrates. High purity HfO_2 ceramic target (99.995%) with diameter of 60 mm and thickness of 5 mm was used as the sputtering target. High purity Ar (99.999%) was introduced into the chamber during deposition. The distance between substrate and target was maintained at 60 mm. The deposition temperature was fixed at room temperature. The base vacuum was higher than 2.0×10^{-4} Pa. Prior to HfO_2 thin film deposition, the target was pre-sputtered in Ar for 5 min to remove the surface oxide of the target. The RF power and the working pressure were fixed at 60W and 0.35 Pa during the sputtering process, respectively. The deposition time was 1.5 h. The Ar flow was kept at 20 SCCM and the O_2 flow changed from 0 to 16 SCCM to make the O_2/Ar flow ratio (R) range from 0 to 0.8. The values of R_1, R_2, R_3 and R_4 are 0, 0.2, 0.4 and 0.8, respectively. Film microstructure has been analyzed by x-ray diffraction (XRD, MXP 18AHF MAC Science, Yokohama, Japan). The X-ray source was Cu-Kα, with an accelerating voltage of 40 kV, a current of 100 mA, scanning range from 20° to 80°, glancing angle of 2°, scanning step of 0.02°, and scanning speed of 8°/min. Fourier transform infrared spectroscopy (FTIR) measurements in the spectral range 400–1200 cm^{-1} are carried out using a Thermo Nicolet MagnaIR 760 spectrophotometer equipped with a deuterated triglycine sulfate detector with KBr windows and an XT-KBr beam splitter, whose measurements resolution was 8 cm^{-1}. The surface morphology of the samples are measured by Hitachi S-4800 type scanning electron microscope (SEM, Hitachi, Tokyo, Japan) and atomic force microscope (AFM, CSPM4000) in contact mode. The optical transmission spectra were measured by UV–vis spectrophotometer (Shimadzu, UV-2550) with wavelength ranging from 190 to 900 nm. In addition, the thickness, refractive index, extinction coefficient and dielectric dispersion of the films were examined and fitted by spectroscopic ellipsometer (SC630, SANCO Co, Shanghai) of the rotating analyzer type. The measurements were carried out in air at room temperature in the wavelength range of 280–1100 nm with a step of 10 nm at an incident angle of 65° and 75°. Al/HfO_2/Si MOS capacitors were fabricated by sputtering a Al top electrode through a shadow mask with an area of 7.065×10^{-4} cm^2 and the back surfaces of all samples were deposited with about 200-nm-thick Al film by sputtering. The *C–V* measurement was obtained by a semiconductor device analyzer (Agilent B1500A) combined with Cascade Probe Station at room temperature. All the electrical characterization was performed at room temperature in a shielded dark box.

3. Results and discussion

3.1. Microstructure and morphology analysis

The structural properties of sputtering-grown HfO_2 thin films were analyzed by XRD. Fig. 1 shows the microstructure of HfO_2 thin film deposited at different O_2/Ar flow ratios. From Fig. 1, it can be noted that orientations of (−111), (111) and (002) appear at $2\theta = 28.3°$, 31.7° and 34.3°, respectively. According to the powder diffraction ICDD card (06–0318), all the peak positions of HfO_2 films correspond to the monoclinic phase and no diffraction peaks from cubic or tetragonal phase have been observed [23]. The peak intensity from (−111) plane is strongest for all the HfO_2 thin films and the peak from (111) plan disappears with introducing O_2. Meanwhile, the intensity of peak from (002) plane decreases with increasing the O_2/Ar flow ratio. It can be noted that in XRD pattern of sputtering-grown HfO_2 thin films grown in Ar and O_2, the dominant peak is (−111) plane, which is in good agreement with Dave's observation [6]. The disappearance of orientation (111) and the intensity decrease of orientation (002) with the increase in the O_2/Ar flow ratio are attributed to the variation of deposition rate and the degraded degree of crystallization. As we know, amorphous state is desirable as potential high-k gate dielectrics in CMOS device application, in which leakage current is lower and suitable for device application. Continuing increasing the O_2/Ar flow ratio to 1.5 shown in Fig. 1, it can be noted that amorphous HfO_2 high-k gate dielectrics have been obtained, indicating that amorphous state can

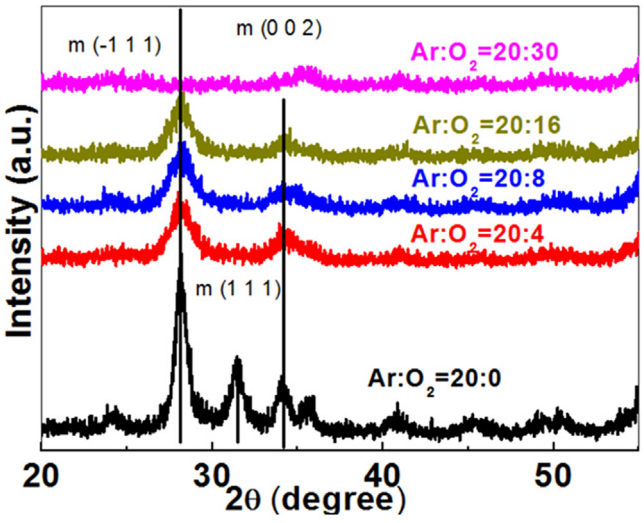

Fig. 1. XRD spectra of sputtering-derived HfO_2 thin films deposited at various O_2/Ar flow ratio.

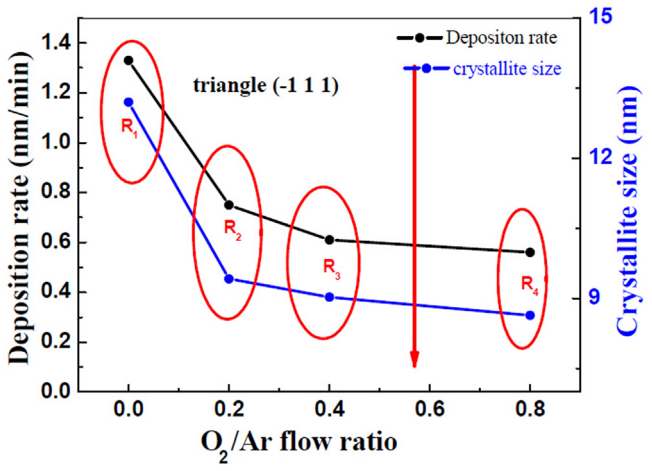

Fig. 2. Deposition rates and crystallite sizes of HfO_2 thin films deposited at various O_2/Ar flow ratio.

be controlled by modulating the oxygen partial pressure.

In order to investigate the oxygen partial pressure dependent evolution of the microstructure for sputtering-derived HfO_2 thin film, the deposition rate and crystallite size also have been calculated, as shown in Fig. 2. Scherrer Equation has been adapted to calculate the average crystallite size as the following formula:

$$D_{hkl} = k\lambda/\beta \cos\theta \quad (1)$$

Where D_{hkl} is the average crystallite size, $k \sim 0.89$ is the shape factor, λ is the wavelength of X-ray, β is full width at half maximum, and θ is diffraction angle. As can be seen in Fig. 2, the deposition rate and crystallite size decreases rapidly as O_2 is introduced into the deposition process. After that, the deposition rate and crystallite size decreases with increasing the O_2/Ar flow ratio. It can be noted that the introduced oxygen reduces the kinetic energy of the sputtered particles, which leads to the suppressed deposition rate. Thus, the crystallite size also decreases with the reduced kinetic energy of the sputtered particles. Meanwhile, higher oxygen flow rate only increases the collision frequency between oxygen molecules and hafnium dioxide particles. So the deposition rate and crystallite size have an apparent reduction. Therefore, it can be concluded that the deposition rate and crystallite size can be modulated by oxygen partial pressure under fixed deposition power.

In order to investigate the evolution of the deposition rate as a function of deposition power, some other experiments have been carried out and new observations have been reported in our previous publication shown in Fig. 3 [17]. Based on our observation, it can be noted that the deposition power plays an important role during deposition process and higher deposition power leads to the formation of HfO_2 films better crystallization. Meanwhile, based on Fig. 3, it can be noted the crystallize size increases slightly as the deposition power increases from 50 to 80 W. Therefore, it can be concluded that deposition power and oxygen partial pressure should be controlled precisely to obtain HfO_2 high-k gate dielectrics with amorphous state.

To further investigate higher oxygen flow rate dependence on the microstructure and interfacial properties of HfO_2 thin films on Si substrates, FTIR measurements have been carried out. Based on Fig. 4, two vibration absorption peaks located at 512 and 610 cm^{-1}, corresponding to the monoclinic phase of HfO_2 film, have been detected, which is in agreement with previous XRD results [24]. The height and the area of vibration absorption peak located at 512 cm^{-1} decrease with increasing the O_2/Ar flow ratio. It is known that the band area is proportional to the concentration of bonds associated to that band [25]. Therefore, these results could indicate that the HfO_2 thickness decreases when the oxygen partial pressure increases.

Fig. 5 shows SEM images of HfO_2 thin films deposited at different O_2/Ar flow ratio. The particle sizes of HfO_2 thin films prepared in pure Ar are larger than those deposited with Ar and O_2. As we know, the Ar flow is kept at 20 SCCM, and the increase of O_2 partial pressure will lead to the reduced Ar ion concentration. Thus, the sputtering yield of HfO_2 reduces and the deposition rate decreases. The thickness of thin films decreases with diminution of the deposition rate. Furthermore, the particle sizes of HfO_2 thin films become smaller and smaller with higher oxygen flow rate. To investigate the surface morphology of the HfO_2 thin films preferably, AFM images shown in Fig. 6 have been used to study the influence of O_2/Ar flow ratio on the surface morphology of HfO_2 thin films. The root mean square (RMS) roughness of the HfO_2 thin films were displayed by raw 2 um × 2um scans. The four samples with O_2 flow rate of 0, 4, 8 and 16 SCCM reveal the root mean square roughness values of 3.39, 1.98, 1.55 and 1.42 nm, respectively. It is noted that surface roughness of HfO_2 thin films prepared in pure Ar is larger that deposited with Ar and O_2. However, surface roughness

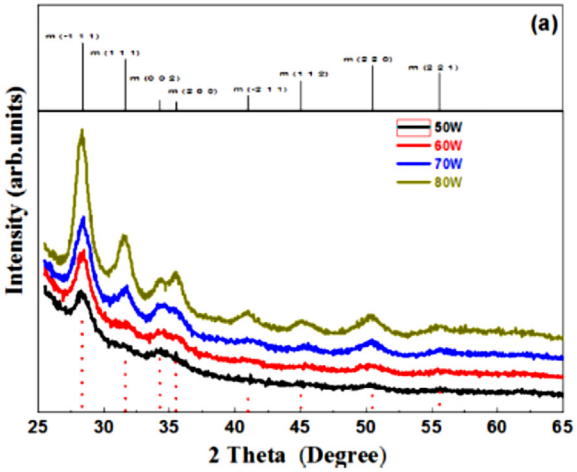

The parameter of HfO_2 thin films by RF magnetron sputtering. **(b)**

Deposition power (W)	Grain sizes (nm)	RMS (nm)	Thickness (nm)	Growth rate (nm/min)
50	8.7	3.0	67.6	0.6
60	9.0	2.9	86.3	0.7
70	9.1	2.8	104.0	0.9
80	9.4	2.1	128.9	1.1

Fig. 3. (a) Deposition-power-dependent XRD spectra of HfO_2 films (a) and (b) calculated deposition parameters.

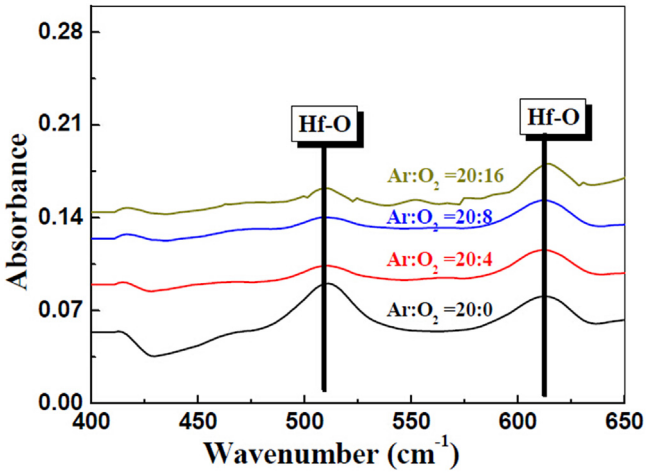

Fig. 4. FTIR spectra for the HfO_2 thin films deposited at various O_2/Ar flow ratio.

values of HfO_2 thin films deposited in Ar and O_2 get smaller and smaller with increasing the O_2/Ar flow ratio, indicating a uniform and smooth surface [26]. The decrease in degree of crystallization produces a decrease in the surface roughness with increasing the O_2/Ar flow ratio. The increase in roughness enhances the hydrophilicity of the surface. But, the HfO_2 thin films deposited in Ar and O_2 with increasing the O_2/Ar flow ratio becomes less hydrophilic. To study the hydrophobicity, static angle measurements were made by dropping 3 μl distilled water on the surface of sample by using sessile drop measurement method. The values of the diameter L and height H are the averages of six measured values. The relation between surface roughness and contact angle is best calculated by flowing Eq [27]:

$$\theta = \arctan\frac{4HL}{L^2 - 4H^2} \tag{2}$$

Where θ is water contact angle, L is the diameter, and H is height of the spherical crown of the droplet dropped on the surface of the HfO_2 films. Fig. 7 shows the variation of water contact angle with increasing the O_2/Ar flow ratio. It can be seen that HfO_2 thin film is a hydrophobic material since its contact angle is greater than 90° as shown in Fig. 7. Then, the contact angle decreases with increasing the O_2/Ar flow ratio. The surface roughness and surface free energy are two main factors governing the surface wettability. However, variation of the initial contact angle of the thin films should be primarily attributed to the difference in their surface roughness according to the previous reports for that the enhancement of hydrophobicity may be ascribed to increase of the proportion of air/water interface in solid and air composite rough surface structure [5,28]. The contact angle decreases with increasing the O_2/Ar flow ratio and the surface roughness also decreases with the increase of the O_2/Ar flow ratio.

3.2. Optical properties analysis

In order to investigate the optical properties of HfO_2 films deposited at various O_2/Ar flow ratio, the optical transmission spectra are shown in Fig. 8. To measure the transmission and absorption spectra of HfO_2 thin films, all the samples were deposited on quartz glass substrates. From Fig. 8, it can be seen that the transmission of all the deposited films in the visible light range (400 nm-900 nm) is more than 75%, indicating that the films have very low absorption in the visible and near ultraviolet region. Meanwhile, with the increase of the oxygen partial pressure, the absorption edges demonstrates an apparent blue shift. Fig. 9 shows absorption spectra of the HfO_2 thin films deposited at different oxygen partial pressure. The energy band gap (E_g) value of the HfO_2 were obtained by absorption spectra and plotting $(\alpha h\nu)^{1/2}$ vs photon energy ($h\nu$) using the following relation [29]:

$$(\alpha h\nu)^{1/2} = A(h\nu - E_g) \tag{3}$$

Where α is the absorption coefficient, A is the constant, and E_g is band gap, respectively. A plot of $(\alpha h\nu)^{1/2}$ vs ($h\nu$) is shown in Fig. 9

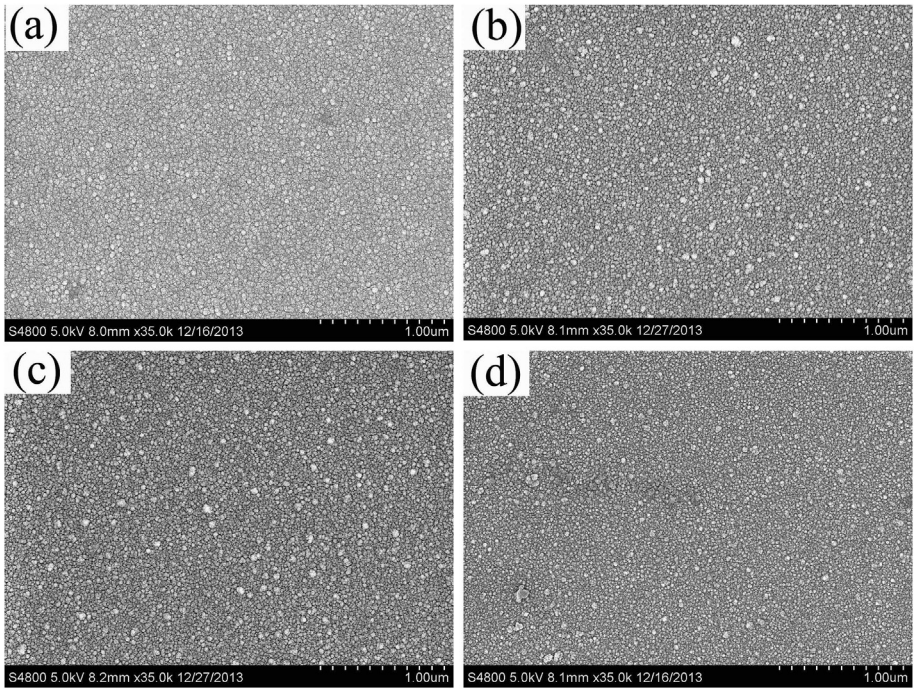

Fig. 5. Surface morphologies of HfO_2 thin films deposited at various O_2/Ar flow ratio: (a) 0; (b) 0.2; (c) 0.4; and (d) 0.8.

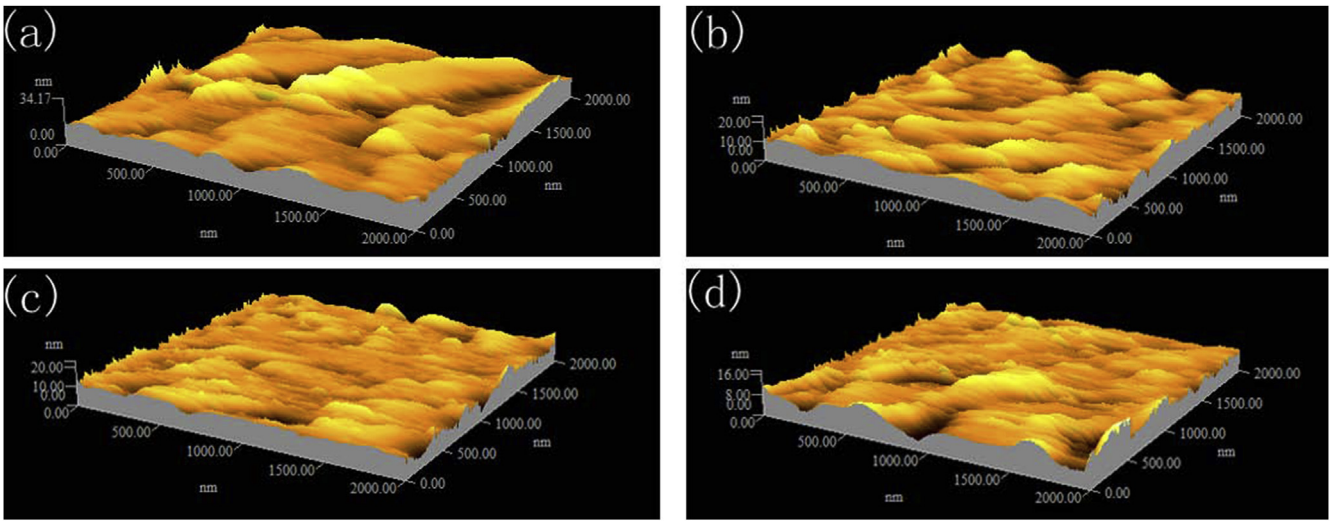

Fig. 6. AFM images of HfO_2 thin films deposited at various O_2/Ar flow ratio: (a) 0; (b) 0.2; (c) 0.4; and (d) 0.8.

and the linear portion of the curve is extrapolated to hν axis to determine the energy band gap. It can be seen clearly that the optical band gap is in the range of 5.58–5.83eV. According to previous reports, band gap energies of 5.41–5.86 eV have been determined for HfO_2 films with monoclinic phase, which is close to our results. As we know, the optical band gap is affected by many factors, such as defects density, purities, packing density, stoichiometric ratio and grain size [30–32]. Based on Fig. 9, the blue shift in optical band gap has been observed with increasing the O_2/Ar flow ratio. Many researchers believe that the quantum size effect results in a dramatic increase in optical band gap energy especially if the crystallite size is less than 30 nm [33,34]. Liu et al. attributed it to the reduction of oxygen vacancy with increasing the O_2/Ar flow ratio [21]. The decrease of packing density and crystallite size are also key factors to result in a dramatic increase in optical band gap energy with increasing the O_2/Ar flow ratio. The packing density and crystallite size have been calculated as shown in Table 1.

An *ex-situ* SE was used to measure O_2 flow rate dependent optical functions of HfO_2 thin films at room temperature in the spectral range of 190–1100 nm. The experimental parameters obtained by SE are the angles Ψ (azimuth) and Δ (phase change), which are related to the microstructure and optical properties, defined by

$$\rho = r_p/r_s = \tan\psi \exp(i\Delta) \quad (4)$$

Where r_p and r_s are the amplitude reflection coefficient for light polarized in the p- and s-planes of incidence, respectively. The spectral dependencies of ellipsometric parameters Ψ (azimuth) and Δ (phase change) can be fitted with appropriate models for the

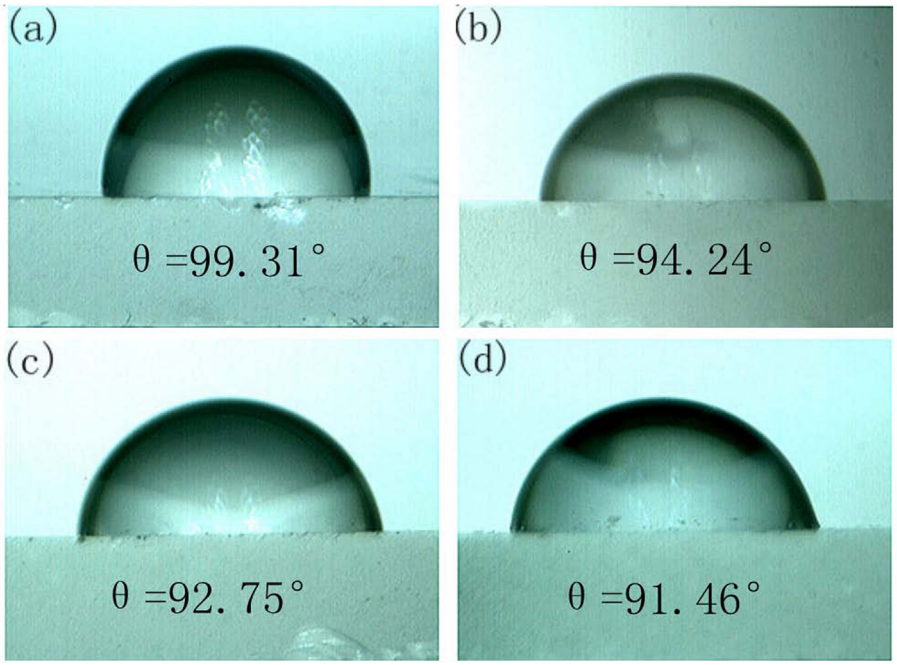

Fig. 7. Variation of contact angle of HfO_2 thin films deposited at various O_2/Ar flow ratio: (a) 0; (b) 0.2; (c) 0.4; and (d) 0.8.

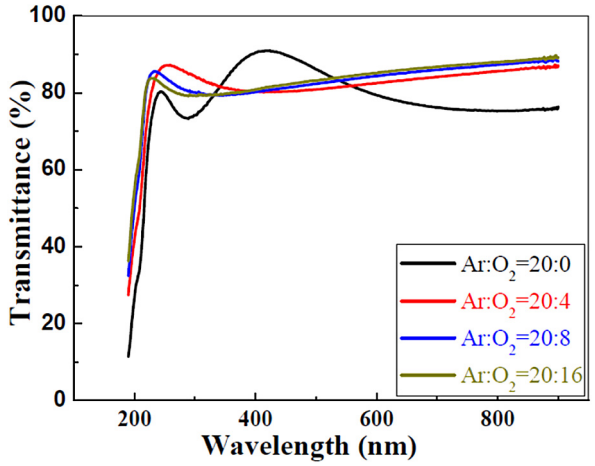

Fig. 8. Transmittance spectra of the HfO_2 thin films deposited at different O2/Ar flow ratio.

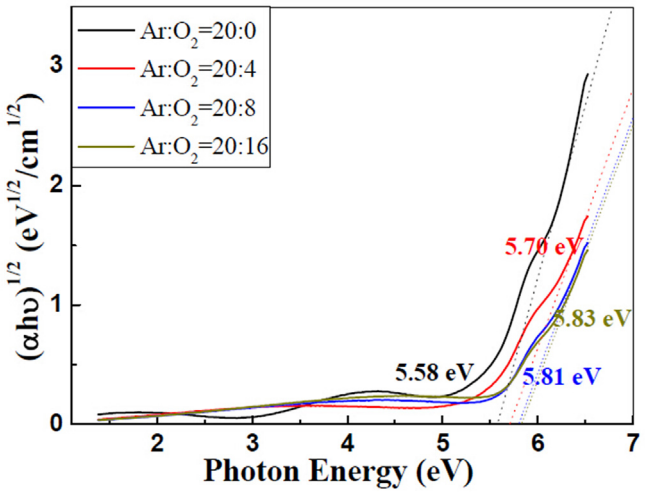

Fig. 9. UV–Vis absorption spectra of the HfO_2 thin films deposited at various O_2/Ar flow ratio.

layer stacking structures and some appropriate optical constant or dispersion model for each layer. When appropriate modeling approaches have been developed, the thickness and the optical properties of the film, such as refractive index n, extinction coefficient k, real (ε_1) and imaginary (ε_2) can be simultaneously extracted from ellipsometric parameters Ψ and Δ. In our SE data analysis, the unknown dielectric function of HfO_2 is described by Cauchy-Urbach model as expressed in the following formulas

$$n(\lambda) = A_n + B_n/\lambda^2 + C_n/\lambda^4 \quad (5)$$

$$k(\lambda) = \delta \exp \beta[12400(1/\lambda - 1/\gamma)] \quad (6)$$

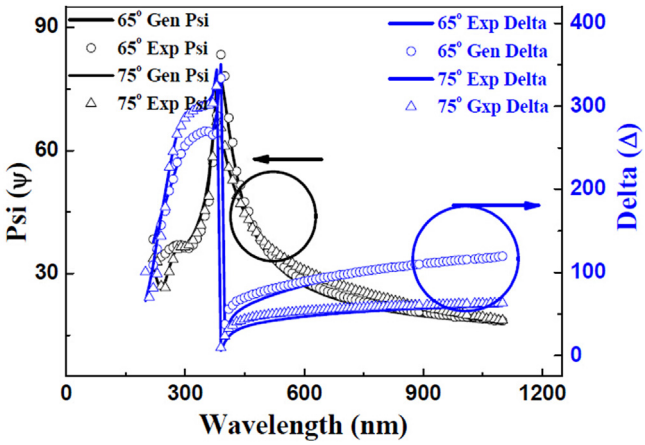

Fig. 10. The experimental and fitted spectroscopy ellipsometry data for HfO_2 film deposited at O_2 flow ratio of 8 SCCM at the incident angle of 65° and 75°.

As we know, Cauchy function is an empirical formula, which was first put forward by A. L. Cauchy. It expresses the material transparent wave dispersion relation. The refractive index n is a graded function changing with wavelength λ and the extinction coefficient k is an exponential function. Above equations as functions of the wavelength λ are uniquely defined by six parameters, An, Bn, Cn, (index parameters which specify the index of refraction). δ, β and γ are the extinction coefficient amplitude, the exponent factor, and the band edge γ, respectively, can be defined as a variable fit parameter during the data evaluation. Thus, using the Cauchy model, the dispersion of optical constants can be described by six parameters. In current work, a three layer model (HfO2/SiO2/Si) has been established to work out the optical function of the HfO2 films related to the O2/Ar flow ratio. The measured and fitted spectra of a representative HfO2 film deposited at O2 flow ratio 8 SCCM at the incident angle of 65° and 75° are shown in Fig. 10. Based on Fig. 10, it can be clearly seen that an excellent agreement between the experimental and fitted spectra for the HfO2 films has been attained in the entirely measured energy range, suggesting that the structured model is reasonable and can describe the structure of the HfO2 thin films. Based on the simplified three-phase model, the best-fitted results used in the simulation of measured spectra are shown in Fig. 10.

Fig. 11 demonstrates the variation of the refractive index and the real part of the dielectric function ε_1 ($\varepsilon_1 = n^2\text{-}k^2$) for the O_2 flow rate of 0, 4, 8 and 16 SCCM. It can be seen that with increasing the O_2/Ar flow ratio, there are an obvious decrease in the value of refractive index. But, Liu et al. [21] reported that the refractive index of thin film decreases when the O_2 is introduced, and then increases with increasing the O_2/Ar flow ratio. As we known, the packing density is decisive factor to affect the value of refractive index. The packing density, p, of a porous film is defined by Yoldas formula as following [35]:

$$p = \left(n_p^2 - 1\right)/n^2 - 1 \quad (7)$$

Table 1
The calculated deposition parameter of sputtering-derived HfO_2 thin films.

Samples	Crystallite size (nm)	Deposition rate (nm/min)	Thickness (nm)	Packing density	RMS roughness (nm)
R_1	13.3	1.32	119.05	0.92	3.39
R_2	9.42	0.75	67.5	0.87	1.98
R_3	9.03	0.62	55.4	0.83	1.55
R_4	8.64	0.56	50.6	0.79	1.42

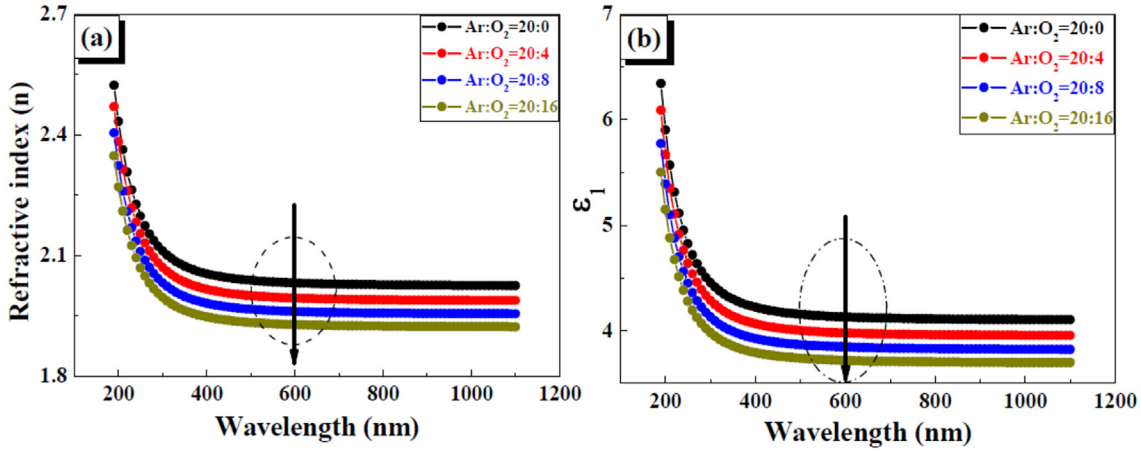

Fig. 11. The calculated refractive index and real parts of the dielectric functions (ε_1) of the HfO_2 films, derived from the results of the Cauchy fitting.

The value of the n (2.1), measured from the material in bulk form, is readily available in the literature. The value of n_p is the refractive index of thin films around 600 nm for all samples. The values of packing density have been calculated as shown in Table 1.The packing density should be related to the thickness of thin films, crystalline structure and crystallite size. Based on Fig. 10(a), the reduction in refractive index has been detected with the increase in oxygen partial pressure, which can be attributed to the reduced packing density. The real part of the dielectric function ε_1 ($\varepsilon_1 = n^2\text{-}k^2$) is similar to n^2 and is related to polarization; the decrease of n indicates the increase of polarization and leads to the reduced dielectric constant, shown in Fig. 11(b).

Fig. 12 shows the extinction coefficient (k) and imaginary ε_2 ($\varepsilon_2 = 2nk$) parts of the dielectric functions of HfO_2 thin films. The extinction coefficient (k) and imaginary ε_2 are close to zero and very low in the visible region. It is noted that the high-quality HfO_2 thin film is obtained for a very small optical loss. The extinction coefficient includes the contribution from the absorption and the scattering of grains. Higher O_2/Ar flow ratios result in the decreased packing density and the size of grains of thin films as shown in Table 1, which brings about the enhancement of scattering effect in HfO_2 thin film. In addition, the blue shift of optical band gap has happened with increasing the O_2/Ar flow ratio, indicating that the optical band gap will increase with increasing the O_2/Ar flow ratio. The absorption coefficient α also can be calculated by the following expression [36]:

$$\alpha = 4\pi k/\lambda \tag{8}$$

Where α is the absorption coefficient, λ is the light wavelength, and k is the extinction coefficient. Then the optical band gap can be calculated by expression (3). The optical band gap has been studied correctly by UV–visible spectroscopy and SE.

In order to investigate optical properties of HfO_2 thin films further, the resultant data of refractive index can be analyzed to obtain the high frequency dielectric constants by applying the following simple classical dispersion relation [37]:

$$\left(n^2 - 1\right) = \left(\frac{s_0\lambda_0^2}{1 - \left(\lambda^2/\lambda_0^2\right)}\right) \tag{9}$$

$$s_0 = \frac{\left(n_0^2 - 1\right)}{\lambda_0^2} \tag{10}$$

Where S_0 is an average oscillator strength and λ_0 is an average oscillator position, n_o is the refractive index at infinite wavelength λ_0 (average interband oscillator wavelength). The plots of $1/n^2-1$ versus $1/\lambda^2$ give straight lines with different slopes and fit the classical dispersion formula with a single electronic oscillator well as shown in Fig. 13. The parameters λ_0 and S_0 can be deduced from the slope $(-1/S_0)$ of the resulting straight line and the infinite

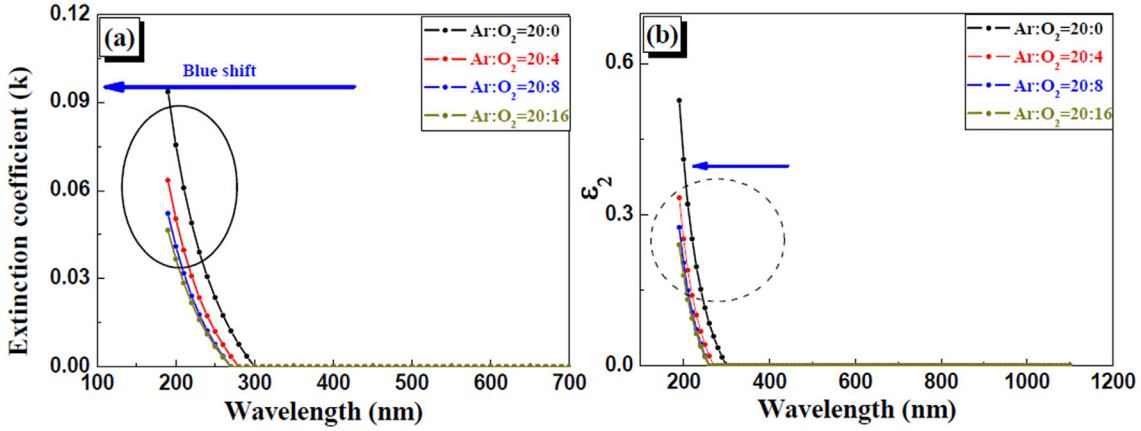

Fig. 12. The extinction coefficient and imaginary parts of the dielectric functions (ε_2) of HfO_2 films deposited at various O_2/Ar flow ratio.

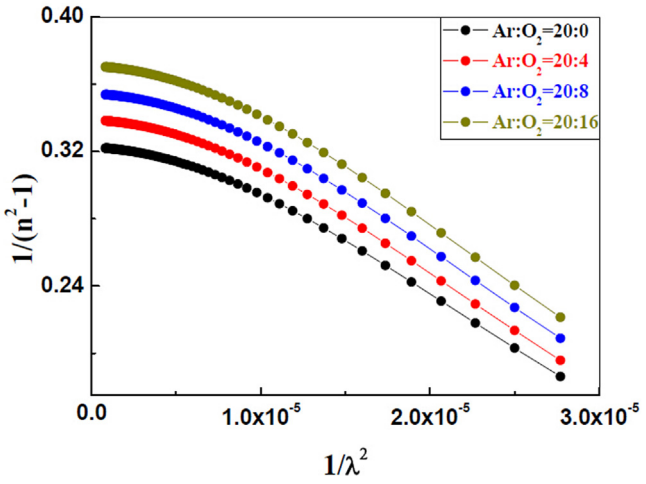

Fig. 13. The plots of $1/(n^2-1)$ vs $1/\lambda^2$ for HfO_2 films deposited at various O_2/Ar flow ratio.

Table 2
Dispersion parameters of the HfO_2 films with various O_2/Ar flow ratio.

Samples	S_o (nm^{-2})	ε_∞	λ_o (nm)
R_1	1.56×10^{-6}	4.03	139
R_2	1.27×10^{-6}	3.82	148
R_3	1.05×10^{-6}	3.63	158
R_4	0.88×10^{-6}	3.38	164

wavelength intercept ($1/S_0\lambda_0^2$), respectively. The high frequency dielectric constant $\varepsilon_\infty = n_0^2$, which depends on the characteristics of the various interband transitions, can also be determined, shown in Table 2. It can be noted that the high frequency dielectric constants decrease with the increased O_2/Ar flow ratio, originating from the decrease of the refractive index of the films.

3.3. Electrical properties analysis

Fig. 14 shows the typical high frequency (1 MHz) *C–V* characteristics of MOS capacitors based on HfO_2 high-k gate dielectrics a functions of oxygen partial pressure. Based on Fig. 14(a), it can be seen that the increased accumulation capacitance and the reduced hysteresis in HfO_2/Si system with increasing the oxygen partial pressure, which may come from the reduced interfacial layer and the improved dielectric constant the dielectric. In addition, the *C–V* measurements for HfO_2/Si always lead a flat band voltage (V_{FB}) shift to the positive direction, suggesting more negative or less positive trapped charges induced in HfO_2. The trend of V_{FB} shift implies that these electrical characteristics could be improved by modulating the oxygen partial pressure. As shown in inset of Fig. 14(b), high gate leakage current density is observed when gate is applied positive voltage for the sample with lower oxygen partial pressure. This is likely due to the interface trap assisted tunneling and/or interfacial oxide induced lowering of conduction band offset. Suppress of the gate leakage current by applying higher oxygen partial pressure is also observed clearly. Based on FTIR analysis, it can be seen that high oxygen partial pressure effectively protects against the oxidation of the substrate and suppress the interfacial layer regrowth, and thus leads to the larger accumulation capacitance, leading to the reduced leakage. Based on previous analysis, it can be inferred that good electrical performance of MOS capacitor based on HfO_2 high-k gate dielectrics can be controlled by modulating the oxygen partial pressure.

4. Conclusions

In summary, the effect of O_2 partial pressure on the microstructure, wettability, and optical and electrical properties of sputtering-derived HfO_2 thin films has been investigated systematically. XRD results have confirmed that the HfO_2 thin films deposited in Ar and O_2 are all polycrystalline with monoclinic phase. Moreover, the crystallite size decreases with the increased O_2/Ar flow ratio. The particle sizes of HfO_2 thin films become smaller and smaller with higher O_2 flow rate confirmed by SEM measurements. AFM analysis shows the RMS of the HfO_2 thin films decreases with increasing the O_2/Ar flow ratio. Meanwhile, the contact angle decreases and the wettability increases with increasing the O_2/Ar flow ratio. The increase in optical band gap and reduction in refractive index with increasing O_2/Ar flow ratio have been detected by UV–Vis and SE measurement. As a result, improved *C–V* characteristics and reduced leakage current have been achieved from MOS capacitors of Al/HfO_2/Si/Al stack with high oxygen partial pressure, which can be attributed to the suppressed interfacial layer and improved interface quality. The precise determination of optical and electrical properties of sputtering-derived HfO_2 thin films paves the way for the application HfO_2-based transition metal oxides in future devices.

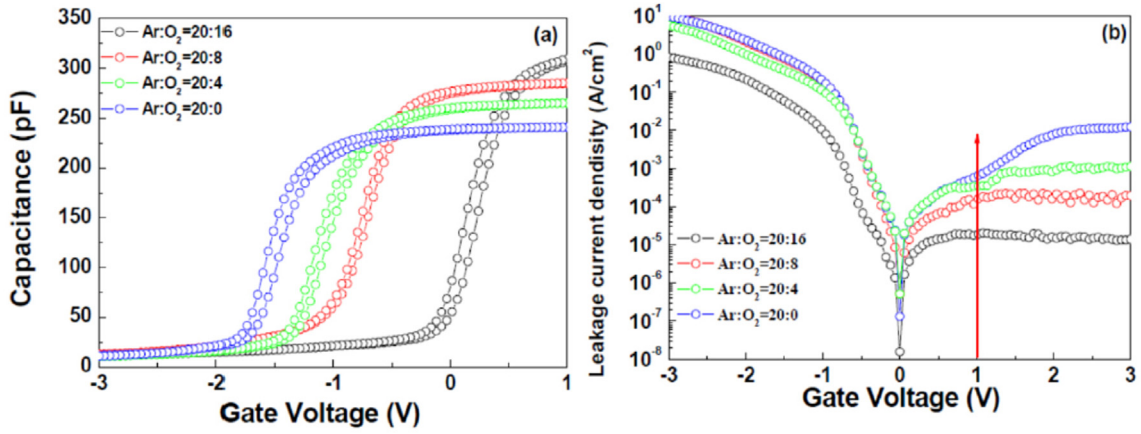

Fig. 14. (a) *C–V* and (b) *I–V* characteristics of MOS capacitors based on HfO_2 high-k gate dielectrics as functions of oxygen partial pressure.

Acknowledgments

The authors acknowledge the support from National Key Project of Fundamental Research (2013CB632705), National Natural Science Foundation of China (51572002,11474284,51472003), Outstanding Young Scientific Foundation and Youth Science Research Foundation of Anhui University (KJJQ1103), and "211 project" of Anhui University.

References

[1] A. Avila-Garcia, M. Garcia-Hipiolito, Characterization of gas sensing HfO_2 coatings synthesized by spray pyrolysis technique, Sens. Actuat. B 133 (2008) 302–307.
[2] G. He, Q. Fang, J.X. Zhang, L.Q. Zhu, M. Liu, L.D. Zhang, Structural, interfacial and optical characterization of ultrathin Zirconia film grown by in-situ thermal oxidation of sputtered metallic Zr films, Nanotechnology 16 (2005) 1641–1647.
[3] L.P. Feng, N. Li, H. Tian, Z.T. Liu, Current conduction mechanisms in HfO_2 and SrHfON thin films prepared by magnetron sputtering, J. Mater. Sci. 49 (2013) 1875–1881.
[4] G. He, X.S. Chen, J.G. Lv, H.S. Chen, B. Deng, Z.Q. Sun, Interface Optimization and Band Alignments of HfTiO/InGaAs Gate Stacks by Metalorganic Chemical Vapor Deposition of AlON Passivation Layer, Sci. Adv. Mater 5 (2013) 1410–1417.
[5] V. Dave, P. Dubey, H.O. Gupta, R. Chandra, Influence of sputtering pressure on the structural, optical and hydrophobic properties of sputtered deposited HfO_2 coatings, Thin Solid Films 549 (2013) 2–7.
[6] V. Dave, P. Dubey, H.O. Gupta, R. Chandra, Effect of sputtering gas on structural, optical and hydrophobic properties of DC-sputtered hafnium oxide thin films, Surf. Coat. Technol. 232 (2013) 425–431.
[7] J.G. Lv, C.L. Liu, W.B. Gong, Z.F. Zi, X.S. Chen, K. Huang, T. Wang, G. He, X.P. Song, Z.Q. Sun, Effect of Surface Topography on Wettability of ZnO Thin Films Deposited by Hydrothermal Method, Sci. Adv. Mater 4 (2012) 757–762.
[8] G. He, B. Deng, Z. Sun, X. Chen, Y. Liu, L. Zhang, CVD-derived Hf-based high-k gate dielectrics, Crit. Rev. Solid. State, Mater. Sci. 38 (2013) 235–261.
[9] M.S. Kim, Y.D. Ko, M. Yun, J.H. Hong, M.C. Jeong, J.M. Myoung, I. Yun, Characterization and process effects of HfO_2 thin films grown by metal-organic molecular beam epitaxy, Mater. Sci. Eng. B 123 (2005) 20–30.
[10] J. Varghese, T. Joseph, M.T. Sebastian, Sol-Gel derived $TiSiO_4$ ceramics for high-k gate dielectric applications, AIP. Conf. Proc. 1372 (2010) 193–197.
[11] J. Zuo, G.G. Nie, X. Gu, Y. Zong, L. Sun, C.J. Lin, Fabrication of TiO_2/Au nanorod arrays employing a positive sacrificial ZnO template and their electrochromic property, Mater. Lett. 61 (2007) 2632–2637.
[12] V. Kapaklis, P. Poulopoulous, V. Karoutsos, T. Manouras, C. Politis, Growth of thin Ag films produced by radio frequency magnetron sputtering, Thin Solid Films 510 (2006) 138–142.
[13] G. He, Q. Fang, L.D. Zhang, Silicate layer formation at HfO_2/SiO_2/Si interface determined by x-ray photoelectron spectroscopy and infrared spectroscopy, J. Appl. Phys. 100 (2006) 083517.
[14] T. Kawahara, M. Yamamuka, T. Makita, J. Naka, A. Yuuki, N. Mikami, K. Ono, Step Coverage and Electrical Properties of (Ba,Sr)TiO_3 Films Prepared by Liquid Source Chemical Vapor Deposition Using $TiO(DPM)_2$, Jpn. J. Appl. Phys. 33 (1994) 5129–5134.
[15] J. Zuo, Deposition of Ag nanostructures on TiO_2 thin films by RF magnetron sputtering, Appl. Surf. Sci. 256 (2010) 7096–7101.
[16] Y.C. Liu, S.K. Tung, J.H. Hsieh, Influence of annealing on optical properties and surface structure of ZnO thin films, J. Cryst. Growth 287 (2006) 105–111.
[17] B. Deng, G. He, J.G. Lv, X.F. Chen, J.W. Zhang, M. Zhang, Z.Q. Sun, Modulation of the structural and optical properties of sputtering-derived HfO_2 films by depostion power, Opt. Mater 37 (2014) 245–250.
[18] X.F. Chen, G. He, M. Liu, J.W. Zhang, B. Deng, P.H. Wang, M. Zhang, J.G. Lv, Z.Q. Sun, Modulation of optical and electrical properties of sputtering-derived amorphous InGaZnO thin films by oxygen partial pressure, J. Alloys Comp. 615 (2014) 636–642.
[19] Z.B. He, W.D. Wu, H. Xu, Y.J. Tang, J.C. Zhang, The effects of O_2/Ar ratio on the structure and properties of hafnium dioxide (HfO_2) films, Vacuum 81 (2006) 211–214.
[20] M. Toledano-Luque, E. San Andrés, J. Oliea, A. del Prado, I. Mártil, W. Bohne, J. Röhrich, E. Strub, Hafnium oxide thin films deposited by high pressure reactive sputtering in atmosphere formed with different Ar/O_2 ratios, Mater. Sci. Semicond. Process 9 (2006) 1020–1024.
[21] W.T. Liu, Z.T. Liu, F. Yan, T.T. Tan, H. Tian, Influence of O_2/Ar flow ratio on the structure and optical properties of sputtered hafnium dioxide thin films, Surf. Coat. Technol. 205 (2010) 2120–2125.
[22] L. Pereira, P. Barquinha, E. Fortunato, R. Martins, Influence of the oxygen/argon ratio on the properties of sputtered hafnium oxide, Mater. Sci. Eng. B 118 (2005) 210–213.
[23] M.F. Al-Kuhaili, S.M.A. Durrani, I.A. Bakhtiari, M.A. Dastageer, M.B. Mekki, Influence of hydrogen annealing on the properties of hafnium oxide thin films, Mater. Chem. Phys. 126 (2011) 515–523.
[24] M. Modreanu, J. Sancho-Parramon, O. Durand, B. Servet, M. Stchakovsky, C. Eypert, C. Naudin, A. Knowles, F. Bridou, M.F. Ravet, Investigation of thermal annealing effects on microstructural and optical properties of HfO_2 thin films, Appl. Sur. Sci. 253 (2006) 328–334.
[25] M. Toledano-Luque, F.L. Martinez, E. San Andres, A. del Prado, I. Martil, G. Gonzalez-Diaz, W. Bohne, J. Rohrich, E. Strub, Physical properties of high pressure reactively sputtered hafnium oxide, Vacuum 82 (2008) 1391–1394.
[26] G. He, Q. Fang, G.H. Li, J.P. Zhang, L.D. Zhang, Structural and optical properties of nitrogen-incorporated HfO_2 gate dielectrics deposited by reactive sputtering, Appl. Sur. Sci. 253 (2007) 8483–8488.
[27] J.G. Lv, K. Huang, X.M. Chen, J.B. Zhu, F.M. Meng, X.P. Song, Z.Q. Sun, Appl. Sur. Sci. 256 (2010) 4720–4723.
[28] W.B. Gong, G.C. Pan, F.J. Shang, F. Wang, Z.T. Zhou, C.L. Liu, M. Zhao, Z.F. Zi, Y.R. Wei, J.G. Lv, X.S. Chen, G. He, M. Zhang, X.P. Song, Z.Q. Sun, Effect of ehylene glycol monomethyl ether ratio in mixed solvent on surface morphology wettability and ptotocatalytic properties of ZnO thin films, J. Mater. Sci. Mater Electron 25 (2014) 2948–2956.
[29] G. He, L.D. Zhang, G.H. Li, M. Liu, X.J. Wang, Structure, composition and evolution of dispersive optical constants of sputtered TiO2 thin films: effect of nitrogen doping, J. Phys. D. Appl. Phys. 41 (2008) 045304.
[30] J. Aarik, H. Mandar, M. Kirm, L. Pung, Optical characterization of HfO_2 thin films grown by atomic layer deposition, Thin Solid Films 466 (2004) 41–47.
[31] Y.J. Cho, W.J. Lee, C.Y. Kim, M.H. Cho, H. Kim, H.J. Lee, D.W. Moon, H.J. Kang, Band gap charge and interfacial reaction in Hf-silicate film grown on Ge(001), J. Chem. Phys. 129 (2008) 164117.
[32] M.C. Cisneros-Morales, C.R. Aita, The effect of nanocrystallite size in monoclinic HfO2 films on lattice expansion and near-edge optical absorption, Appl. Phys. Lett. 96 (2010) 191904.
[33] K. Xiong, J. Robertson, Point defects in HfO_2 high K gate oxide, Microelectron. Eng. 80 (2005) 408–411.
[34] Y.B. Zheng, S.J. Wang, A.C.H. Huan, C.Y. Tan, L. Yan, C.K. Ong, Al_2O_3-incorporation effect on the band structure of $Ba_{0.5}Sr_{0.5}TiO_3$ thin films, Appl. Phys. Lett. 86 (2005) 112910.
[35] S.M.A. Durrani, CO-sensing properties of hafnium oxide thin films prepared by electron beam evaporation, Sens. Actuat. B 120 (2007) 700–705.
[36] G. He, L.D. Zhang, G.W. Meng, G.H. Li, G.T. Fei, X.J. Wang, J.P. Zhang, M. Liu, Q. Fang, Ian W. Boyd, Composition dependence of electronic structure and optical properties of $Hf_{1-x}Si_xO_y$ gate dielectrics, J. Appl. Phys. 104 (2008) 104116.
[37] G. He, L.D. Zhang, M. Liu, J.P. Zhang, X.J. Wang, C.M. Zhen, Thickness-modulated optical dielectric constant and band alignments of HfO_xN_y gate dielectrics, J. Appl. Phys. 105 (2009) 014109.